PROCEEDINGS OF SPIE

Applications of Digital Image Processing XLIII

Andrew G. Tescher
Touradj Ebrahimi
Editors

24 August – 4 September 2020
Online Only, United States

Sponsored and Published by
SPIE

Volume 11510

Part One of Two Parts

Proceedings of SPIE 0277-786X, V. 11510

Applications of Digital Image Processing XLIII, edited by Andrew G. Tescher,
Touradj Ebrahimi, Proc. of SPIE Vol. 11510, 1151001 · © 2020 SPIE
CCC code: 0277-786X/20/$21 · doi: 10.1117/12.2581642

The papers in this volume were part of the technical conference cited on the cover and title page. Papers were selected and subject to review by the editors and conference program committee. Some conference presentations may not be available for publication. Additional papers and presentation recordings may be available online in the SPIE Digital Library at SPIEDigitalLibrary.org.

The papers reflect the work and thoughts of the authors and are published herein as submitted. The publisher is not responsible for the validity of the information or for any outcomes resulting from reliance thereon.

Please use the following format to cite material from these proceedings:
Author(s), "Title of Paper," in *Applications of Digital Image Processing XLIII*, edited by Andrew G. Tescher, Touradj Ebrahimi, Proceedings of SPIE Vol. 11510 (SPIE, Bellingham, WA, 2020) Seven-digit Article CID Number.

ISSN: 0277-786X
ISSN: 1996-756X (electronic)

ISBN: 9781510638266
ISBN: 9781510638273 (electronic)

Published by
SPIE
P.O. Box 10, Bellingham, Washington 98227-0010 USA
Telephone +1 360 676 3290 (Pacific Time) · Fax +1 360 647 1445
SPIE.org

Printed in the United States of America by Curran Associates, Inc., under license from SPIE.

Publication of record for individual papers is online in the SPIE Digital Library.

SPIE. DIGITAL LIBRARY
SPIEDigitalLibrary.org

Paper Numbering: *Proceedings of SPIE* follow an e-First publication model. A unique citation identifier (CID) number is assigned to each article at the time of publication. Utilization of CIDs allows articles to be fully citable as soon as they are published online, and connects the same identifier to all online and print versions of the publication. SPIE uses a seven-digit CID article numbering system structured as follows:

- The first five digits correspond to the SPIE volume number.
- The last two digits indicate publication order within the volume using a Base 36 numbering system employing both numerals and letters. These two-number sets start with 00, 01, 02, 03, 04, 05, 06, 07, 08, 09, 0A, 0B … 0Z, followed by 10-1Z, 20-2Z, etc. The CID Number appears on each page of the manuscript.

Multiparametric polarization histology in the detection of traumatic changes in the optical anisotropy of biological tissues

Litvinenko, A., Garazdyuk, M., Bachinsky, V., Vanchulyak, O., Ushenko, A., et al.

A. Litvinenko, M. Garazdyuk, V. Bachinsky, O. Vanchulyak, A. Ushenko, Yu. Ushenko, A. Dubolazov, P. Gorodensky, O. Yatsko, Bin Lin, Zhebo Chen, "Multiparametric polarization histology in the detection of traumatic changes in the optical anisotropy of biological tissues," Proc. SPIE 11510, Applications of Digital Image Processing XLIII, 115102O (21 August 2020); doi: 10.1117/12.2568408

SPIE.

Event: SPIE Optical Engineering + Applications, 2020, Online Only

Multiparametric polarization histology in the detection of traumatic changes in the optical anisotropy of biological tissues

A.Litvinenko[1], M. Garazdyuk[1], V. Bachinsky[1], O. Vanchulyak[1], A.Ushenko[2] Yu.Ushenko[2], A.Dubolazov[2*], P.Gorodensky[2], O.Yatsko[2], Lin Bin[3], Chen Zhebo[3]

[1] Bukovinian State Medical University, 3 Theatral Sq., Chernivtsi, Ukraine, 58000
[2] Chernivtsi National University, 2 Kotsiubynskyi Str., Chernivtsi, Ukraine, 58012
[3] Reasearch Institute of Zhejiang University-Taizhou, 38 Zheda Road, Hangzhou, People's Republic of China, Zhejiang Province, 310027

a.dubolazov@chnu.edu.ua

ABSTRACT

For a high-precision objective histological determination of the prescription of damage to internal organs over a long period of time, a systematic approach was used based on digital azimuthally invariant polarizing, Mueller-matrix and tomographic methods for studying temporary changes in the molecular and polycrystalline structure of brain, liver and kidney samples in the post-mortal period.
It was revealed that a linear change in the magnitude of statistical moments of the 1st - 4th orders characterizing the distribution of data of digital azimuthally invariant polarizing, Mueller-matrix and tomographic methods is interconnected with the duration of damage to internal organs. On this basis, a new algorithm for digital histological determination of the prescription of the occurrence of damage is proposed.
To determine the extent of damage, the method of azimuthally invariant polarization microscopy with different magnification of the image of histological sections of tissues of internal organs was used, which provided diagnostic relationships between changes in the magnitude of statistical moments of the 1st to 4th orders, which characterize the azimuth and elliptic polarization maps of digital microscopic images and time intervals of damage duration.
Keywords: polarization, biological tissues, optical anisotropy, Mueller matrix, diagnostics.

1. DIFFERENTIAL DIAGNOSIS OF THE LIMITATION OF THE FORMATION OF DAMAGE TO THE INTERNAL ORGANS OF A PERSON BY MAPPING MAPS OF AZIMUTH OF POLARIZATION

Maps of azimuth of polarization of microscopic images of histological sections of the kidney and histograms of the distribution of its magnitude are illustrated by a series of fragments of fig. 1[1-4].

Applications of Digital Image Processing XLIII, edited by Andrew G. Tescher, Touradj Ebrahimi, Proc. of SPIE Vol. 11510, 115102O · © 2020 SPIE
CCC code: 0277-786X/20/$21 · doi: 10.1117/12.2568408

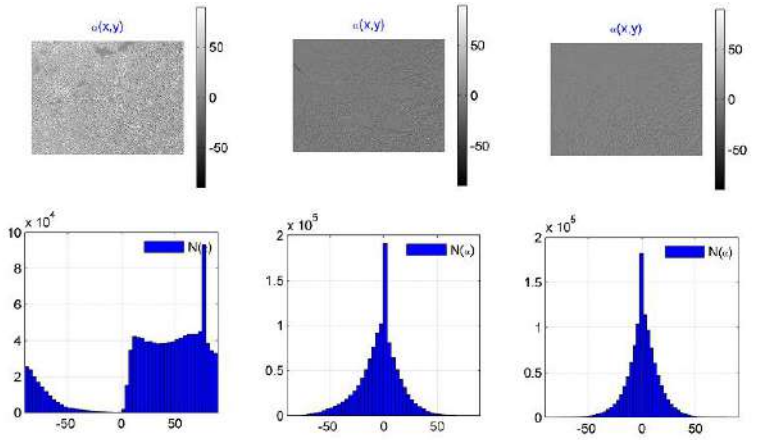

Fig. 1. Maps ((1), (2), (3)) and histograms ((4), (5), (6)) of the distribution of the azimuth of polarization of microscopic images (x4) of histological sections of the kidney of the dead from the control group ((1), (4)), research groups with different damage durations (6 hours - (2), (5)) and (18 hours - (3), (6)).

The statistical structure (Fig. 1, (4) - (6)) of polarization maps (Fig. 1 (1) - (3)) of the images of samples of histological sections of the kidney is less developed compared with the same parameters of the samples of the brain and liver from the control and experimental groups - the average values and dispersion variance are insignificant and decrease with increasing damage duration - 6 hours. (fragment (5)) and 18 hours (fragment (6)), respectively (table 1)[5-15].

Table 1. Temporal dynamics of changes in statistical moments of the 1st - 4th orders of magnitude characterizing the distribution of the PA value of microscopic images (4x) of histological sections of the kidney

T, hours	**2**	**4**	**6**	**12**	**18**
SM_1	0,29 ± 0,017	0,25 ± 0,016	0,24 ± 0,017	0,27 ± 0,015	0,23 ± 0,014
p	p ϕ 0,05				
SM_2	0,29 ± 0,017	0,25 ± 0,016	0,24 ± 0,017	0,27 ± 0,015	0,23 ± 0,014
p	p ϕ 0,05				
SM_3	0,63 ± 0,031	0,78 ± 0,033	0,93 ± 0,042	1,24 ± 0,061	1,29 ± 0,064
p	p π 0,05				p ϕ 0,05
SM_4	0,49 ± 0,022	0,71 ± 0,34	0,92 ± 0,044	1,33 ± 0,055	1,39 ± 0,055
p	p π 0,05				p ϕ 0,05
T, hours	**24**	**30**	**36**	**42**	**48**
SM_1	0.25 ± 0,013	0,24 ± 0,012	0,22 ± 0,011	0,19 ± 0,012	0,17 ± 0,011
p	p ϕ 0,05				
SM_2	0,21 ± 0,012	0,19 ± 0,011	0,17 ± 0,009	0,16 ± 0,009	0,18 ± 0,009
p	p ϕ 0,05				
SM_3	1,34 ± 0,071	1,38 ± 0,074	1,41 ± 0,077	1,49 ± 0,081	1,54 ± 0,087
p	p ϕ 0,05				
SM_4	1,42 ± 0,074	1,46 ± 0,076	1,53 ± 0,083	1,65 ± 0,085	1,64 ± 0,091
p	p ϕ 0,05				

It was established (table 1) that, as diagnostic parameters for identifying the age of kidney damage with polarization mapping of the polarization azimuth, one can use a statistically significant linear change in the magnitude of the

statistical moments of the 3rd (asymmetry - dynamic range 0.61) and 4th (excess - dynamic range 0.84) orders within 12 hours after damage.

Similar data from polarization mapping of large-scale (40x) microscopic images of histological sections of the kidney are presented in fragments of fig. 2.

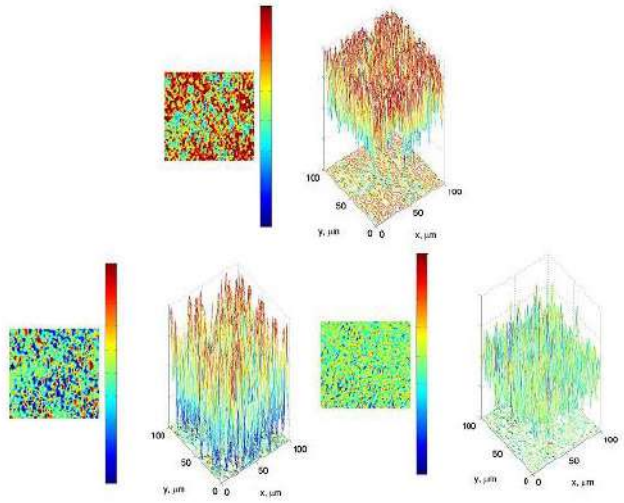

Fig. 2. Maps ((1), (2), (3)) and coordinate distributions ((4), (5), (6)) polarization azimuth values of microscopic images (x40) of histological sections of the kidneys of the dead from the control group ((1), (4)), research groups with different damage durations (6 hours - (2), (5)) and (18 hours - (3), (6)).

A comparative analysis (with mapping data of polarization maps at a magnification of 4, - fig. 1) of the coordinate and fluctuation structures of large-scale maps of the azimuth of polarization of kidney images (as in the case of digital polarization histological studies of brain and liver samples) revealed an increase in the range (fig. 2, fragments (2), (4), (6)) and coordinate heterogeneity (fig. 2, fragments (1), (3), (5)) of the azimuth value variations, - table 2[16-21].

Table 2. Temporal dynamics of changes in the statistical moments of the 1st - 4th orders characterizing the distribution of the PA value of microscopic images (40x) of histological sections of the kidney

T, hours	**2**	**4**	**6**	**12**	**18**
SM_1	0,22 ± 0,017	0,21 ± 0,016	0,19 ± 0,017	0,17 ± 0,015	0,18 ± 0,014
p	p ϕ 0,05				
SM_2	0,17 ± 0,017	0,11 ± 0,016	0,12 ± 0,017	0,09 ± 0,015	0,07 ± 0,014
p		p π 0,05	p ϕ 0,05		
SM_3	0,88 ± 0,031	1,06 ± 0,033	1,21 ± 0,042	1,54 ± 0,061	1,92 ± 0,064
p	p π 0,05				
SM_4	0,71 ± 0,022	0,83 ± 0,34	0,96 ± 0,044	1,23 ± 0,055	1,46 ± 0,055
p	p π 0,05				
T, hours	**24**	**30**	**36**	**42**	**48**
SM_1	0.16 ± 0,09	0,14 ± 0,08	0,12 ± 0,07	0,13 ± 0,08	0,12 ± 0,07
p	p ϕ 0,05				
SM_2	0,08 ± 0,005	0,09 ± 0,006	0,07 ± 0,004	0,05 ± 0,003	0,06 ± 0,004
p	p ϕ 0,05				
SM_3	2,04 ± 0,12	1,98 ± 0,11	2,09 ± 0,13	2,19 ± 0,15	2,11 ± 0,12

p	$p \phi 0{,}05$				
SM_4	$1{,}52 \pm 0{,}08$	$1{,}58 \pm 0{,}09$	$1{,}66 \pm 0{,}11$	$1{,}73 \pm 0{,}11$	$1{,}81 \pm 0{,}12$
p	$p \phi 0{,}05$				

Analysis of the results of statistical processing of large-scale azimuth maps of polarization of microscopic images of histological sections of the kidneys of all groups revealed the following group of parameters that are suitable for detecting the duration of damage:

- time interval of 6 hours (dynamic range 0.06) - dispersion of the variance of the azimuth of polarization of microscopic images;
- time interval of 18 hours. - asymmetry (dynamic range 1.04) and excess (dynamic range 0.75) of azimuth distribution;
- for all other intervals, a temporary change in the magnitude of the statistical moments of the 1st – 4th orders that characterize the polarization structure of large-scale images of histological sections of intact and damaged kidneys is statistically unreliable ($p \phi 0{,}05$).

2. DIFFERENTIAL DIAGNOSIS OF THE LIMITATION OF THE FORMATION OF DAMAGE TO INTERNAL ORGANS OF A PERSON BY THE METHOD OF MAPPING MAPS OF POLARIZATION ELLIPTICITY

In a series of fragments of fig. 3 and table 3 show the results of polarization mapping of the distribution of the ellipticity of digital microscopic images of histological sections of the kidney with different damage durations and statistical analysis of the temporal dynamics of changes in the average, dispersion, asymmetry and excess of polarization maps.

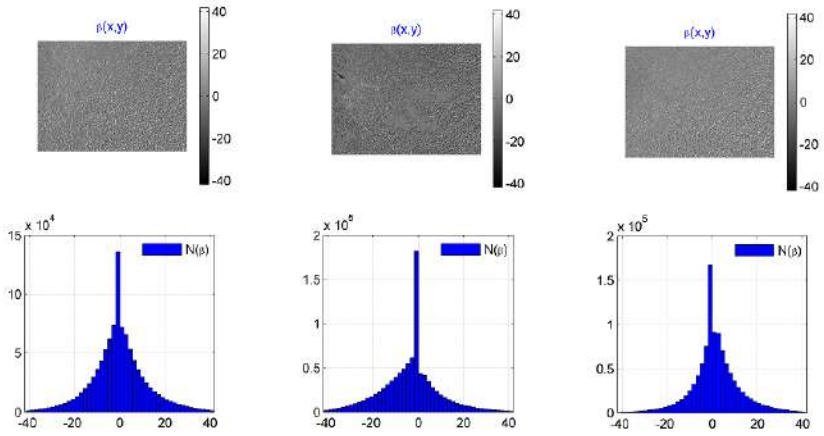

Fig. 3. Maps ((1), (2), (3)) and histograms ((4), (5), (6)) of the distribution of the magnitude of the ellipticity of polarization of microscopic images (x4) of histological sections of the kidney of the dead from the control group ((1), (4)), research groups with different damage durations (6 hours - (2), (5)) and (18 hours - (3), (6)).

Patterns similar to the data of digital polarization histology of brain and liver samples have been established.:

- coordinate heterogeneity of the aggregate of polarization ellipticity maps (fig. 3 (1) - (3) small-scale (4x) microscopic images of intact and damaged kidney samples;
- decrease of the range of variation of random values of the polarization ellipticity at the points of digital microscopic images of histological sections of the kidney from all the studied groups.

Table 3. Temporal dynamics of changes in statistical moments of the 1st - 4th orders characterizing the distribution of the magnitude of the PE of microscopic images (4x) of histological sections of the kidney

T, hours	**2**	**4**	**6**	**12**	**18**
SM_1	$0{,}09 \pm 0{,}005$	$0{,}08 \pm 0{,}013$	$0{,}07 \pm 0{,}004$	$0{,}08 \pm 0{,}005$	$0{,}07 \pm 0{,}004$
p	$p \phi 0{,}05$				
SM_2	$0{,}11 \pm 0{,}006$	$0{,}105 \pm 0{,}006$	$0{,}09 \pm 0{,}005$	$0{,}08 \pm 0{,}005$	$0{,}07 \pm 0{,}004$
p	$p \phi 0{,}05$				
SM_3	$0{,}71 \pm 0{,}032$	$0{,}85 \pm 0{,}036$	$0{,}99 \pm 0{,}041$	$1{,}31 \pm 0{,}069$	$1{,}36 \pm 0{,}062$
p	$p \pi 0{,}05$				$p \phi 0{,}05$
SM_4	$1{,}42 \pm 0{,}071$	$1{,}72 \pm 0{,}81$	$2{,}03 \pm 0{,}091$	$2{,}68 \pm 0{,}12$	$2{,}79 \pm 0{,}13$
p	$0{,}27 \pm 0{,}012$				$0{,}36 \pm 0{,}016$
T, hours	**24**	**30**	**36**	**42**	**48**
SM_1	$0.06 \pm 0{,}003$	$0{,}04 \pm 0{,}002$	$0{,}02 \pm 0{,}001$	$0{,}03 \pm 0{,}002$	$0{,}02 \pm 0{,}001$
p	$p \phi 0{,}05$				
SM_2	$0{,}08 \pm 0{,}005$	$0{,}055 \pm 0{,}003$	$0{,}03 \pm 0{,}002$	$0{,}04 \pm 0{,}002$	$0{,}03 \pm 0{,}002$
p	$p \phi 0{,}05$				
SM_3	$1{,}44 \pm 0{,}078$	$1{,}55 \pm 0{,}082$	$1{,}64 \pm 0{,}083$	$1{,}73 \pm 0{,}091$	$1{,}68 \pm 0{,}085$
p	$p \phi 0{,}05$				
SM_4	$2{,}84 \pm 0{,}14$	$2{,}86 \pm 0{,}16$	$2{,}73 \pm 0{,}15$	$2{,}84 \pm 0{,}16$	$2{,}74 \pm 0{,}15$
p	$p \phi 0{,}05$				

The results are shown in table 3, for different times ago kidney damage was found:

- almost all changes in the magnitude of the statistical moments of the 1st - 4th orders are statistically unreliable ($p \phi 0{,}05$);
- in the time range with a limitation of up to 12 hours the statistical moments of the 3rd (dynamic range 0.61) and 4th (dynamic range 1.24) orders characterizing the asymmetry and excess of distributions of the polarization ellipticity.

In fig. 4 shows maps of polarization ellipticity and coordinate distribution of fluctuations of its magnitude in the plane of large-scale (40x) microscopic images of histological sections of the kidney.

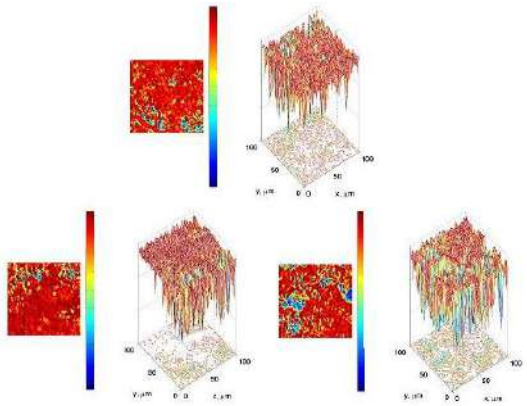

Fig. 4. Maps ((1), (2), (3)) and coordinate distributions ((4), (5), (6)) the magnitude of the ellipticity of polarization of microscopic images (x40) of histological sections of the kidneys of the dead from the control group ((1), (4)), research groups with different damage durations (6 hours - (2), (5)) and (18 hours - (3), (6)).

Table 4. Temporal dynamics of changes in the statistical moments of the 1st - 4th orders characterizing the distribution of the magnitude of the PE of microscopic images (40x) of histological sections of the kidney

T, hours	**2**	**4**	**6**	**12**	**18**
SM_1	0,08 ± 0,005	0,07 ± 0,004	0,06 ± 0,004	0,07 ± 0,005	0,06 ± 0,004
p	p ϕ 0,05				
SM_2	0,09 ± 0,004	0,06 ± 0,003	0,05 ± 0,003	0,04 ± 0,002	0,05 ± 0,003
p		p π 0,05	p ϕ 0,05		
SM_3	0,97 ± 0,043	1,31 ± 0,063	1,64 ± 0,071	2,27 ± 0,105	2,93 ± 1,42
p	p π 0,05				
SM_4	1,84 ± 0,071	2,09 ± 0,09	2,34 ± 0,11	2,84 ± 0,12	3,29 ± 0,15
p	p π 0,05				
T, hours	**24**	**30**	**36**	**42**	**48**
SM_1	0.06 ± 0,003	0,04 ± 0,002	0,02 ± 0,001	0,03 ± 0,002	0,02 ± 0,001
p	p ϕ 0,05				
SM_2	0,05 ± 0,003	0,055 ± 0,003	0,03 ± 0,002	0,04 ± 0,002	0,03 ± 0,002
p	p ϕ 0,05				
SM_3	3,11 ± 0,16	3,25 ± 0,17	3,36 ± 0,17	3,39 ± 0,17	3,44 ± 0,18
p	p ϕ 0,05				
SM_4	3,38 ± 0,14	3,49 ± 0,16	3,31 ± 0,16	3,39 ± 0,16	3,14 ± 0,15
p	p ϕ 0,05				

Quantitatively, the transformation of the statistical structure of polarization ellipticity maps in the form of temporal dynamics of changes in statistical moments of the 1st to 4th orders of magnitude characterizing the distribution of the magnitude of the PE of microscopic images (40x) of histological sections of the kidney is presented in table 4.

The following diagnostic intervals and parameters for detecting kidney damage were established.:

- 18 hours - statistically significant (p π 0,05) a change in the magnitude of the statistical moments of higher orders (asymmetries - the dynamic range of 1.45 and excess - the dynamic range of 1.96) of the distribution of the magnitude of the polarization ellipticity;
- 6 hours — linear and statistically significant (p π 0,05) change (dynamic range 0.03) of the dispersion of the distribution of polarization ellipticity.

3. TIME INTERVALS AND ACCURACY OF THE POLARIZATION MAPPING METHOD

Table 5. Time intervals and accuracy of the polarization mapping method of the maps of azimuth of polarization

Brain				
Statistical moments	Interval, hours		Accuracy, min.	
Magnification	4x	40x	4x	40x
Average	_	_	_	–
Dispersion	_	_	_	–
Asymmetry	12	18	60	55
Excess	12	18	60	55
Liver				
Statistical moments	Interval, hours		Accuracy, min.	
Magnification	4x	40x	4x	40x
Average	_	_	_	_

Dispersion	_	_	_	–
Asymmetry	12	18	70	60
Excess	12	18	70	60
Kidney				
Statistical moments	Interval, hours		Accuracy, min.	
Magnification	4x	40x	4x	40x
Average	_	_	_	–
Dispersion	_	_	_	–
Asymmetry	12	18	65	60
Excess	12	18	65	60

Table 6. Time intervals and accuracy of the method of polarization mapping of maps of polarization ellipticity

Brain				
Statistical moments	Interval, hours		Accuracy, min.	
Magnification	4x	40x	4x	40x
Average	_	_	_	_
Dispersion	_	_	_	_
Asymmetry	12	18	70	60
Excess,	12	18	70	60
Liver				
Statistical moments	Interval, hours		Accuracy, min.	
Magnification	4x	40x	4x	40x
Average	_	_	_	_
Dispersion	_	_	_	_
Asymmetry	12	18	80	70
Excess	12	18	80	70
Kidney				
Statistical moments	Interval, hours		Accuracy, min.	
Magnification	4x	40x	4x	40x
Average	_	_	_	_
Dispersion	_	_	_	_
Asymmetry	12	18	75	65
Excess	12	18	75	65

CONCLUSIONS

1. The azimuthally invariant polarization techniques of digital histology of samples of human internal organs (kidney) with different damage durations of 1 hour up to 120 hours was experimentally tested.
2. The scenarios of changing the statistical structure of the azimuth and polarization ellipticity maps of microscopic images of histological sections of the internal organs of a person are determined - with an increase in the duration of the damage, the average and dispersion decrease, the asymmetry and excess increase.
3. The following ranges of linear change in the variation of the magnitude of statistical indicators of polarizing digital histology and the accuracy of determining the duration of damage:
   3.1. Maps of azimuth of polarization of microscopic images with a magnification of 4x:

- asymmetry – 12 hours;
- excess – 12 hours
- accuracy 60 min. – 70 min.

3.2. Maps of azimuth of polarization of microscopic images with a magnification of 40x:

- asymmetry – 12 hours;
- excess – 12 hours
- accuracy – 55 min. – 60 min.

3.3. Maps of ellipticity of polarization of microscopic images with a magnification of 4x:

- asymmetry – from 12 hours;
- excess – 12 hours
- accuracy - 70 min. – 80 min.

3.4. Maps of ellipticity of polarization of microscopic images with a magnification of 40x:

- asymmetry – 12 hours;
- excess – 12 hours
- accuracy – 65 min. – 75 min.

REFERENCES

[1]. Wang X. Propagation of polarized light in birefringent turbid media: a Monte Carlo study / X. Wang, L.-H. Wang // J. Biomed. Opt. – 2002. – Vol. 7. – P. 279-290.

[2]. Tuchin V. V. Handbook of optical biomedical diagnostics / V. V. Tuchin. – Bellingham : SPIE Press, 2002. – 1110 p.

[3]. Yao G. Two-dimensional depth-resolved Mueller matrix characterization of biological tissue by optical coherence tomography / G. Yao, L. V. Wang // Opt. Lett. – 1999. – V. 24. – P. 537-539.

[4]. Tower T. T. Alignment Maps of Tissues: I. Microscopic Elliptical Polarimetry / T. T. Tower, R. T. Tranquillo // Biophys. J. – 2001. – Vol. 81. – P. 2954-2963.

[5]. Lu S. Interpretation of Mueller matrices based on polar decomposition / S. Lu, R. A. Chipman // J. Opt. Soc. Am. A. –1996. – Vol. 13. – P.1106-1113.

[6]. Ghosh Nirmalya. Techniques for fast and sensitive measurements of two-dimensional birefringence distributions / Nirmalya Ghosh, I. Alex Vitkin // Journal of Biomedical Optics. – 2011. – № 16(11). – P. 110801.

[7]. V. V. Tuchin, L. Wang, and D. A` . Zimnyakov, Optical Polarization in Biomedical Applications, New York, USA (2006).

[8]. Angelsky, O.V., Maksimyak, A.P., Maksimyak, P.P., Hanson, S.G., "Optical correlation diagnostics of rough surfaces with large surface inhomogeneities," Optics Express, 14 (16), 7299-7311(2006).

[9]. Ushenko, A.G., "Correlation Processing and Wavelet Analysis of Polarization Images of Biological Tissues," (2001) Optics and Spectroscopy (English translation of Optika i Spektroskopiya), 91 (5), pp. 773-778.

[10]. Ushenko, A.G., Ermolenko, S.B., Burkovets, D.N., Ushenko, Yu.A., "Polarization microstructure of laser radiation scattered by optically active biotissues," (1999) Optika i Spektroskopiya, 87 (3), pp. 470-474.

[11]. Angelsky, O. V., Bekshaev, A. Y. A., Maksimyak, P. P., Maksimyak, A. P., & Hanson, S. G. (2018). Low-temperature laser-stimulated controllable generation of micro-bubbles in a water suspension of absorptive colloid particles. Optics Express, 26(11), 13995-14009.

[12]. Angelsky, O. V. (2007). Optical correlation techniques and applications. Optical correlation techniques and applications (pp. 1-270)

[13]. Angelsky, O. V., Ushenko, A. G., Pishak, V. P., Burkovets, D. N., Yermolenko, S. B., Pishak, O. V., & Ushenko, Y. A. (2000). Coherent introscopy of phase-inhomogeneous surfaces and layers. Paper presented at the Proceedings of SPIE - the International Society for Optical Engineering, 4016 413-418.

[14]. Angelsky OV, Bekshaev AY, Hanson SG, Zenkova CY, Mokhun II and Jun Z (2020) Structured Light: Ideas and Concepts. Front. Phys. 8:114.

[15]. Angelsky OV, Zenkova CY, Hanson SG and Zheng J (2020) Extraordinary Manifestation of Evanescent Wave in Biomedical Application. Front. Phys. 8:159.

[16]. Ushenko, Yu.A., Bachynsky, V.T., Vanchulyak, O.Ya., Dubolazov, A.V., Garazdyuk, M.S., Ushenko, V.A., "Jones-matrix mapping of complex degree of mutual anisotropy of birefringent protein networks during the differentiation of myocardium necrotic changes," (2016) Applied Optics, 55 (12), pp. B113-B119.

[17]. Ushenko, Yu.A., Dubolazov, A.V., Karachevtcev, A.O., Zabolotna, N.I., "A fractal and statistic analysis of Mueller-matrix images of phase inhomogeneous layers,"(2011) Proceedings of SPIE - The International Society for Optical Engineering, 8134, 81340P.

[18]. Ushenko, V.A., Dubolazov, A.V., "Correlation and self similarity structure of polycrystalline network biological layers mueller matrices images," (2013) Proceedings of SPIE - The International Society for Optical Engineering, 8856.

[19]. "Cassidy, "Basic concepts of statistical analysis for surgical research," Journal of Surgical Research 128,199-206 (2005).

[20]. C. S. Davis, Statistical methods of the analysis of repeated measurements, 744, New York: Springer-Verlag (2002).

[21]. A. Petrie, B. Sabin, Medical Statistics at a Glance, pp. 157, Blackwell Publishing (2005).